

# Electrodeposition of Zn-Fe Alloy from an Acid Sulfate Bath Containing Triethanolamine

by V. Narasimhamurthy and B.S. Sheshadri

**Electrodeposition of Zn-Fe alloy from an acid sulfate bath containing triethanolamine (TEA) under optimized plating conditions, such as pH, temperature, stirring, current density, and metal ion ratios in the bath, the TEA concentration produced desired alloy compositions of 15–20 wt percent of Fe. An alloy of this composition exhibited superior corrosion resistance, high hardness, and a smooth, uniform, fine-grained deposit, with improved cathodic current efficiency. An alloy containing more than 40 wt percent Fe showed good paintability characteristics. The structure of the electrodeposited alloy is correlated with electrochemical properties. The mechanism of alloy deposition is discussed.**

In the past 20 years, many efforts have been directed to development of high-corrosion-resistance steel, especially for automotive body panels.<sup>1-4</sup> Recently, electrodeposited zinc-iron alloys have been shown to be most suitable for this purpose.<sup>5-7</sup>

Zinc-iron alloy deposits can provide sacrificial protection to steel, even up to 85 wt percent Fe. An alloy containing 15–25 wt percent Fe gives excellent corrosion resistance, formability, weldability, workability, and adaptability to phosphating and chromating. An alloy deposit containing more than 40 wt percent Fe has been shown to have excellent paintability. The Zn-Fe alloy deposits have been reported to offer corrosion protection to steel superior to pure zinc.<sup>5</sup>

In this study, the authors developed a new bath that provides good leveling action and throwing power for depositing Zn-Fe alloy deposits having a composition of 15–25 wt percent Fe. The results reported here also contain the plating variables, and include studies of phase structure, composition, electrochemical behavior and corrosion in salt solution.

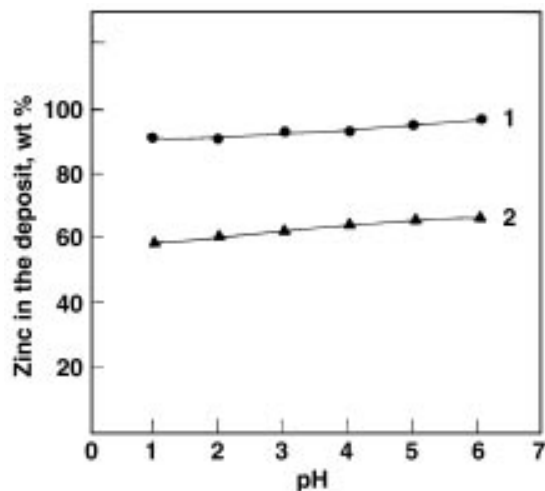


Fig. 1—Effect of pH on the wt percent of zinc in the alloy deposit. Bath composition: 156 g/L  $ZnSO_4 \cdot 7H_2O$ , 178 g/L  $(NH_4)_2SO_4 \cdot FeSO_4 \cdot 7H_2O$ , 14 mL/L TEA, 20 g/L  $Na_2SO_4$ , 30 g/L  $H_3BO_3$ , 3.52 g/L ascorbic acid, 50 mg/L sodium lauryl sulfate, temp 50 °C, CD 15 mA/cm<sup>2</sup> and thickness 6  $\mu$ m. 1. Zn/Fe 80/20 2. Zn/Fe 90/10.

## Experimental Procedure

The sequence of plating operations followed, and the bath composition developed for the study, are given in Tables 1 and 2, respectively. The electrolyte contains analytical-grade chemicals dissolved in deionized water, with the pH of the plating solution adjusted to the desired value. The electrolyte was purified as described elsewhere.<sup>8</sup>

Hull cell experiments were carried out in a standard 267-mL cell for 5 min at 1 A cell current. The test results were used to optimize the plating parameters. The percentage of zinc and iron in the deposit was determined by plating onto a stainless steel cathode having an area of 1 cm<sup>2</sup>. The panel so plated was weighed, then stripped in 20-percent  $HNO_3$  and made up to 100 mL in a standard flask.

Zinc and iron concentrations in the solution were estimated by atomic absorption spectroscopy. No baking was done after plating.

The cathode current efficiencies (CCE) and the deposition rate were calculated in the conventional manner. During plating, the potential was recorded with reference to a standard calomel electrode, using a digital voltmeter.

The effect of plating variables—pH, current density, temperature, ligand concentration, metal ion ratio, and agitation—on the composition of the alloy deposit and on the CCE were studied. The thickness of the deposit was measured by

Table 1  
Sequence of Plating Operations

1. Mechanical polish
2. Degrease in trichloroethylene
3. Pickle in 10% HCl for one min
4. Rinse
5. Alkali dip
6. Rinse
7. Acid dip
8. Rinse
9. Plate

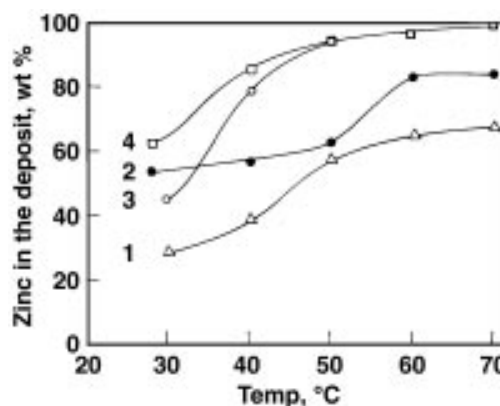


Fig. 2—Effect of temp on percentage of zinc in the alloy deposit. Bath composition as in Fig. 1; pH 4 and thickness 6  $\mu$ m. 1. Zn/Fe 90/10, CD 20 mA/cm<sup>2</sup> 2. Zn/Fe 80/20, CD 20 mA/cm<sup>2</sup> 3. Zn/Fe 90/10, CD 10 mA/cm<sup>2</sup> 4. Zn/Fe 80/20, CD 10 mA/cm<sup>2</sup>.

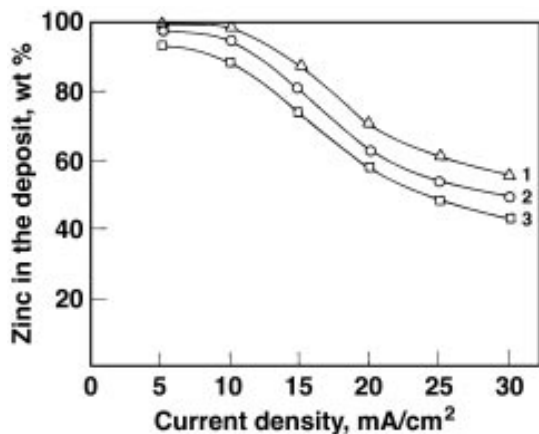


Fig. 3—Effect of CD on percentage of zinc in the deposit. Bath as in Fig. 1; pH 4, Temp 50 °C and thickness 6  $\mu\text{m}$ . 1. 0.025 M TEA 2. 0.1 M TEA 3. 0.6 M TEA.

Elicometer.<sup>a</sup> The coated Zn-Fe alloy (8  $\mu\text{m}$ ) deposits on steel were tested for corrosion resistance by an accelerated neutral salt spray test as per ASTM B117 by using 5 percent NaCl and compared with pure zinc coating of same thickness on steel.

Polarization studies were made using a potentiostat/galvanostat<sup>b</sup> in the current density range 0–100 mA/cm<sup>2</sup>, using 1 cm<sup>2</sup> cathode area of the sample, exposed to 5-percent NaCl solution. Microhardness of the alloy deposits were measured with a 100-g load<sup>c</sup> for alloys containing various wt percentages of Fe.

Paintability of the alloy deposits with different percentages of iron were determined by cross-hatching method. The phase and crystal structure of the deposit were determined by powder X-ray diffraction with a diffractometer.<sup>d</sup> The surface morphology of the alloy deposit was examined under a scanning electron microscope (SEM). The paint used was a synthetic enamel known as Opolite.

## Results and Discussion

### Effect of pH

Variation of the percentage of zinc content in the deposit with the pH is shown in Fig. 1. The wt percent of zinc in the deposit remains constant with increase in the bath pH. This is expected only if the deposition potential of the metal complex in the bath does not change with pH. Smooth, uniform deposits with desired alloy composition are obtained by operating the bath at an optimum pH of 4.0.

### Effect of Temperature

The optimum temperature required to produce a smooth, uniform deposit was found to be 50 °C. Temperature above 50 causes precipitation of undesirable insoluble ferric hy-

<sup>a</sup> Model 256 FN (UK).

<sup>b</sup> Model CL-95 (Elico, India)

<sup>c</sup> Zwick 32122 (Germany)

<sup>d</sup> JEOL-JDX-8P (Japan)

<sup>e</sup> Model JEOL JSM-840A (Japan)

Table 2  
Plating Bath Compositions

Components	Zn/Fe-10/90	20/80	30/70	40/60	50/50	60/40
ZnSO <sub>4</sub> · 7H <sub>2</sub> O	0.05	0.10	0.15	0.20	0.20	0.30
(NH <sub>4</sub> ) <sub>2</sub> SO <sub>4</sub> · FeSO <sub>4</sub> · 6H <sub>2</sub> O	0.45	0.40	0.35	0.30	0.25	0.20

0.025–0.60 M TEA, 0.02 M ascorbic acid, 20 g/L Na<sub>2</sub>SO<sub>4</sub>, 30 g/L H<sub>3</sub>BO<sub>3</sub>, 50 mg/L sodium lauryl sulfate.

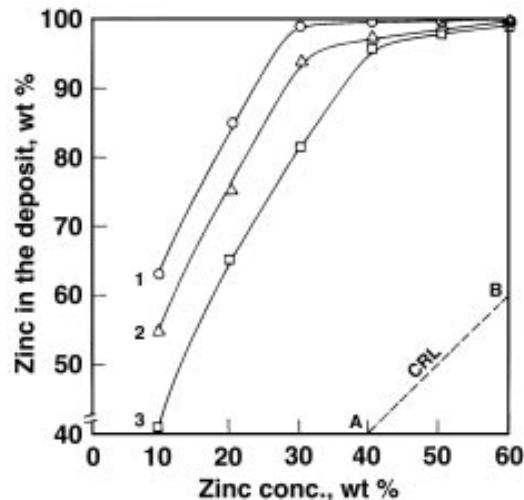


Fig. 4—Effect of Zn/Fe ratio on percentage of zinc in the alloy deposit. Bath as in Fig. 1; pH 4, temp 50 °C, CD 20 mA/cm<sup>2</sup> and thickness 6  $\mu\text{m}$ . 1. 0.1 M TEA 2. 0.6 M TEA 3. 0.025 M TEA.

droxide and degraded products of ligands that interfere with the rate of deposition and decrease CCE. At temperatures below 50 °C the rate of plating was limited, which causes more Fe inclusion in the alloy deposit. Figure 2 illustrates the variation of alloy composition with bath temperature, showing that with increase in temperature, there is an increase in zinc content in the deposit; this is a typical case of anomalous co-deposition. At elevated temperature, an increase in the concentration of zinc metal in the cathode diffusion layer might be expected, which favors enhanced deposition of metal that was already being deposited preferentially; accordingly, the process was classified as anomalous codeposition.<sup>9</sup>

### Effect of Current Density

Figure 3 indicates that with increase in current density, the wt percent of zinc in the alloy deposit decreases. At higher current densities, with the less noble zinc being preferentially deposited, a zinc hydroxide film forms at the cathode. The film must be relatively more depleted in zinc than iron. As a result, the alloy that was under diffusion control (anomalous) takes on the character of normal alloy plating; consequently, the zinc content in the alloy deposit shows a downward trend with increase in current density. Deposits with 15–25 wt percent Fe obtained between 10–20 A/ft<sup>2</sup> were adherent, smooth, uniform and finer grained. Therefore, the optimum current density was fixed as 10–20 A/ft<sup>2</sup>.

Table 3  
Effect of Temperature on Cathode Current Efficiency and Percentage Weight in the Alloy Deposit

Temp °C	Wt % Zn	Cathode Current Efficiency %
30	62.54	99
40	85.92	84
50	94.16	78
60	96.93	75
70	99.13	62

Bath: Zn<sup>2+</sup>, 0.1 M; Fe<sup>2+</sup>, 0.4 M; TEA, 0.1 M; ascorbic acid, 0.02 M; Na<sub>2</sub>SO<sub>4</sub>, 20 g/L; H<sub>3</sub>BO<sub>3</sub>, 30 g/L; pH 4.0, CD 10 mA/cm<sup>2</sup>, thickness 6  $\mu\text{m}$ ; sodium lauryl sulfate, 50 mg/L.

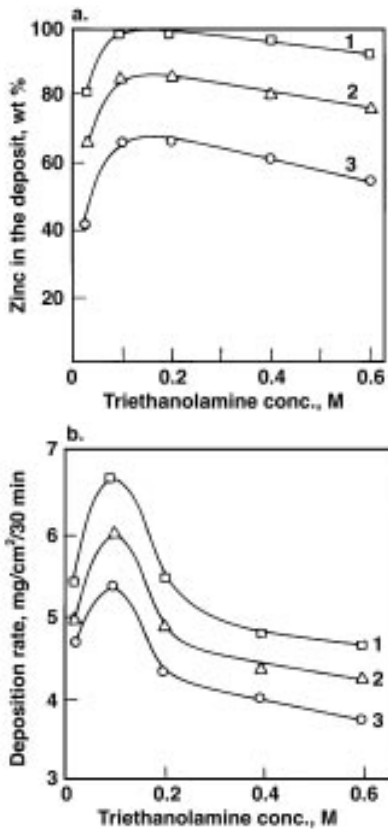


Fig. 5—Effect of TEA concentration on percentage of zinc in the alloy deposit and the deposition rate: (a) effect on composition; (b) effect on deposition rate. Bath as in Fig. 1, temp 50 °C, pH 4, CD 20 mA/cm<sup>2</sup> and thickness 6 μm. 1. Zn/Fe 90/10 2. Zn/Fe 80/20 3. Zn/Fe 70/30.

to that in the deposit. A bath solution with less zinc in the bath and containing a definite concentration of TEA, was found to produce a zinc-rich alloy. As a result, zinc deposits preferentially, although it is less noble than iron, and the process is classified as anomalous codeposition. This behavior is attributed to the formation of zinc hydroxide film on the cathode surface because of the rise in pH around the cathode film. This film suppresses the deposition of iron.<sup>10</sup>

#### Effect of TEA Concentration

TEA was found to be a suitable complexing agent for both zinc and iron, and is stable up to pH 6.<sup>11</sup> Figure 5a illustrates

Table 4  
Hardness and Static Potentials of Alloy Deposits

Alloy	Hardness VHN (100 g)	Static Potential mV vs. SCE
Zn	80	-1078
Zn-5% Fe	122	-1041
Zn-10% Fe	135.9	-1001
Zn-15% Fe	139.0	-954
Zn-20% Fe	145.2	-914
Zn-25% Fe	152.4	-882
Zn-30% Fe	157.5	-845
Zn-35% Fe	164.1	-807
Zn-40% Fe	172.0	-754
Mild steel	—	-700

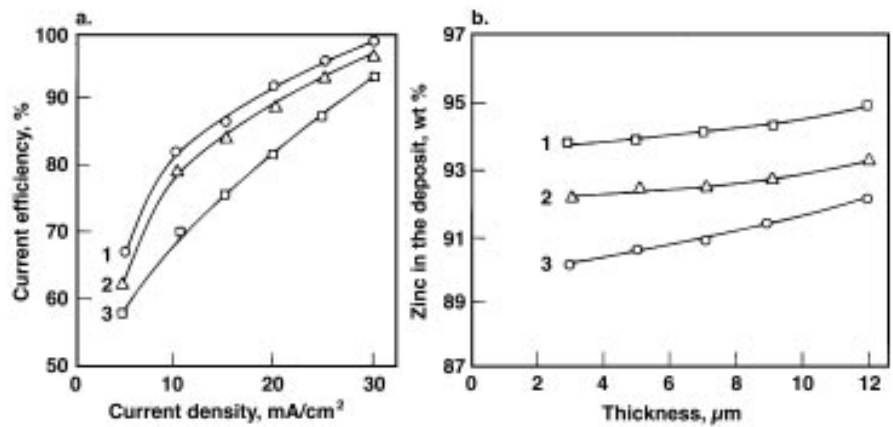


Fig. 6—(a) Effect of CD on CCE: Bath as in Fig. 1, pH 4, temp 50 °C and thickness 6 μm. 1. 0.025 M TEA 2. 0.1 M TEA 3. 0.6 M TEA. (b) effect of thickness on percentage of zinc in the alloy deposit: CD 20 mA/cm<sup>2</sup>. 1. 0.1 M TEA, 2. 0.6 M TEA 3. 0.025 M TEA.

#### Effect of Metal Ion Ratio

The ratio of zinc to iron in the bath, in principle, influences the composition of the alloy deposit. Figure 4 illustrates the effect of the metal ion ratio in the bath on alloy composition. The line AB is the composition reference line (CRL), which represents the metal ratio in the bath, which is equal

the variation of alloy composition with TEA concentration. The amount of zinc in the deposit increased with increase in TEA concentration to a maximum value, then decreased slightly with further increase in the amount of TEA. The maximum zinc content in the deposit was observed at a TEA concentration of 0.1 M. This is probably because zinc might form a loose complex with the TEA rather than with iron at this concentration, which facilitates discharge of more zinc ions. At a higher TEA concentration, however, the slight decrease in zinc content in the deposit probably results from formation of a stronger complex of zinc with TEA, hindering the smooth discharge of zinc ions and causing a decrease in wt percent.

Figure 5b shows the dependence of deposition rate on TEA concentration. The deposition rate initially increases sharply with TEA and reaches a maximum at a TEA concentration of 0.1 M. Beyond this, the deposition rate falls with further increase in TEA concentration. Other alloy systems studied in the presence of TEA showed maximum deposition rates in the range of 0.1 to 0.2 M of TEA.<sup>12,13</sup>

#### Effect of Agitation

With agitation of the plating solution, the formation of insoluble ferric hydroxide can be reduced, increasing the iron content in the deposit, thereby increasing the CCE.

Table 5  
Electrochemical Corrosion Parameters (Polarization Study) of Electrodeposited Zinc and Zinc Alloy Coatings on Steel

Wt % Zn	Coating Thickness 8 μm			
	Corrosion potential mV vs. SCE	Corrosion current density j(μA/cm <sup>2</sup> )	Corrosion rate milli-in. per yr	Polarization resistance kΩ/cm <sup>2</sup>
Pure Zn	-1078	98	116.64	0.764
95	-1076	50	58.77	1.830
90	-1070	45	52.25	5.430
85	-1065	26	29.80	6.420
80	-1042	10	11.82	9.321
75	-1020	30	33.55	7.980
70	-1001	35	36.17	6.850
65	-940	49	53.45	5.812
60	-938	90	96.96	0.620

Potentiodynamic scans were made at 0.166 mV/sec in an aerated, stirred 5% NaCl solution, pH 6, 25 ± 2 °C.

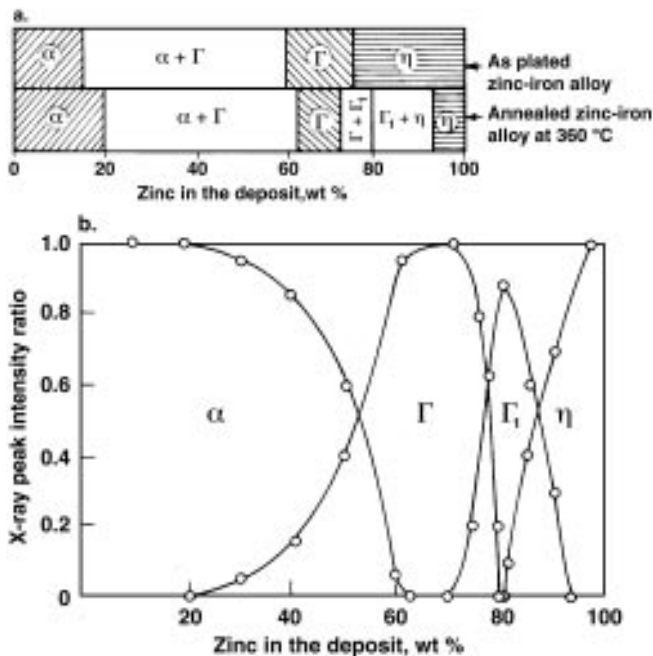


Fig. 7—(a) Constitution diagram of electrodeposited zinc-iron vs. percent of zinc in the alloy deposit; (b) phase composition of electrodeposited zinc-iron alloy vs. percentage of zinc in the alloy deposit.

#### Cathodic Current Efficiency (CCE)

The CCE of Zn-Fe baths is mainly dependent on ferric ion concentration, organic impurities, the types of stabilizers and additives used, and on the plating variables. Ferric ion concentration influences the rate of deposition by reducing CCE. Temperature is also another factor that contributes to reduction in efficiency in dilute solution, as indicated in Table 3. Figure 6a illustrates the effect of current density on CCE. Increase in current density increases the Fe content in the alloy deposit and decreases the CCE.

#### Effect of Thickness

Figure 6b shows the variation of alloy composition with thickness of the deposit. The wt percent of zinc in the deposit obtained from a bath containing 0.25 to 0.6 M TEA was almost constant throughout the deposit.

#### Structure and Properties

Phase diagrams of thermally prepared Zn-Fe alloys have been reported earlier.<sup>14-16</sup> The phase structure of electrodeposited Zn-Fe alloy deposits have been determined, however, by X-ray diffraction and are shown in Fig. 7. It also shows the phases identified in the constitution diagram of Zn-Fe alloy. The electrodeposited Zn-Fe alloy has metastable structures and the individual phases co-exist over a wide range of composition. These are:  $\eta$  (100–79 wt % Zn),  $\Gamma$  (79–20 wt % Zn),  $\Gamma_1$  (93–74 wt % Zn) and  $\alpha$  (62–0 wt % Zn). The phase diagram of as-plated Zn-Fe alloy has been compared with annealed alloy at 360 °C. The feature of interest in this diagram is that the solid solubility of zinc in iron ( $\alpha$ -phase) is limited to 20 wt percent Zn in the pure form and extends up to 62 wt percent Zn, along with  $\Gamma$ -phase. The range of co-existence of  $\alpha$ -phase was much longer in the as-plated alloy samples than in the equilibrium alloy (annealed). The  $\Gamma$ -phase exists in a range up to 79 wt percent Zn. An alloy containing more than 93 wt percent Zn showed pure  $\eta$ -phase. The  $\eta$  and  $\Gamma_1$  phases coexist, however, between 79–93 wt

Table 6  
Optimum Bath Composition and Operating Conditions

Component	Concentration/units g/L
ZnSO <sub>4</sub> · 7H <sub>2</sub> O	156
(NH <sub>4</sub> ) <sub>2</sub> SO <sub>4</sub> · FeSO <sub>4</sub> · 7H <sub>2</sub> O	178
Triethanolamine	14 mL/L
Na <sub>2</sub> SO <sub>4</sub>	20
H <sub>3</sub> BO <sub>3</sub>	30
Ascorbic acid	3.52
Sodium lauryl sulfate	50 mg/L
pH	4.0
Temp	50 °C
Current density	15 mA/cm <sup>2</sup>
Agitation	normal

percent Zn. The  $\Gamma_1$  phase does not appear in the as-plated alloys. Accordingly, the electrodeposited alloy exists in the form of intermetallic phases for different percentages of zinc in the alloy deposit.

Figure 8 shows how the surface morphology changes with increase in Fe content in the deposit. The Zn-Fe alloy deposit morphology was compared with the morphology of a pure zinc deposit. Deposits containing 20 wt percent Fe were found to have granular structure.

The microhardness of a 25- $\mu$ m thick alloy deposit is shown in Table 4. As expected, the increased Fe content in the alloy deposit enhanced the hardness.

Adhesion of paint on a Zn-Fe deposit was evaluated after test panels were soaked in deionized water at 40 °C for 240 hr and cross-hatched after drying. The proportion of paint removed was measured after applying adhesive tape to the cross-hatched area and removing it quickly. The paint loss over the cross-hatched area was plotted against wt percent Fe in the alloy deposit. Figure 9 shows that there was no paint loss from a deposit containing 40 wt percent Fe or higher. Alloy deposits containing less than 30 wt percent Fe were inferior in paint adhesion.

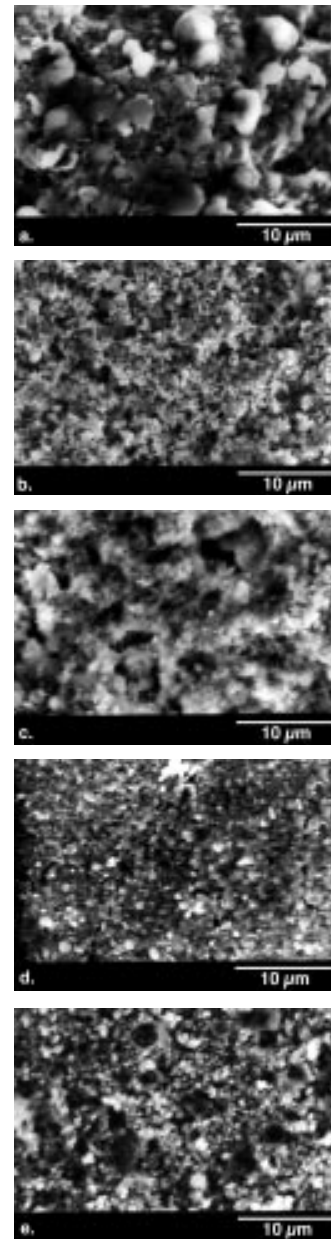


Fig. 8—SEM photographs of alloy deposits (wt % Fe): (a) 0; (b) 10; (c) 15; (d) 20; (e) 30.

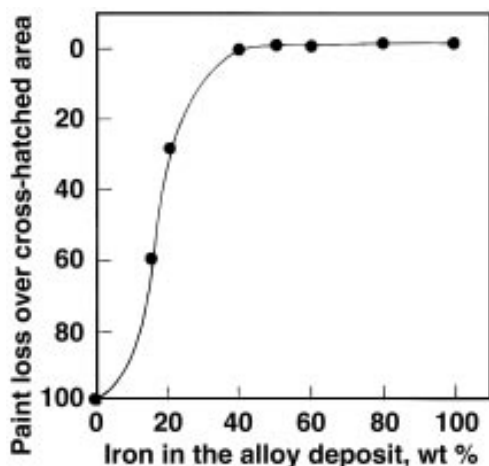


Fig. 9—Effect of Fe content on adhesion of paint.

#### Corrosion Resistance Studies

The static potentials of Zn-Fe alloy was measured in 5-percent NaCl solution. Table 4 shows that the static potential of alloys was significantly more positive to zinc and more negative to steel under identical experimental conditions. This indicates that Zn-Fe alloy can electrochemically protect steel from corrosion.

Alloying zinc with 15–25 wt percent Fe greatly improves its corrosion resistance. This superior corrosion resistance property is one of the major objectives in recent efforts to expand commercial Zn-Fe alloy plating. Substantial improvements are made with a small percentage of iron in the alloy, which replaces zinc and provides enhanced corrosion protection of steel.<sup>17</sup>

Corrosion testing of zinc and Zn-Fe 8- $\mu$ m-thick deposits were carried out by subjecting them to accelerated neutral salt spray testing for 96 hr per ASTM B117 in a 5-percent NaCl solution at 35  $\pm$  2 °C. The alloy samples were compared with pure zinc-coated panels. On the zinc-plated panels, a white corrosion product of zinc was observed after 35 hr, it was followed by red corrosion products of steel after 45 hr. Moreover, none of these panels withstood corrosion for more than 50 hr. On the Zn-Fe alloy coated panels, blisters of white and red rust were noted only after 90 hr, indicating that Zn-Fe alloy coatings protect steel from corrosion more efficiently than pure zinc coatings. The Zn alloy containing 15–25 wt percent Fe showed excellent corrosion resistance to both white and red rust.

#### Electrochemical Polarization

Potentiodynamic polarization studies with alloys containing different proportions of Zn and Fe were carried out on as-plated samples to evaluate the actual corrosion rate, corrosion current density and polarization resistance for coatings on steel. Table 5 lists the electrochemical corrosion parameters measured on zinc alloy coatings. The potentials were recorded with reference to a standard calomel electrode. There was a significant increase in corrosion rate and a decrease in polarization resistance with a pure zinc-coated sample. Very low corrosion current, low corrosion rate and high polarization resistance were observed with Zn-Fe alloy containing 15–25 wt percent Fe.

#### Findings

Zinc-iron alloy containing 15–25 wt percent Fe electroplated from an acid sulfate bath containing TEA were morphologi-

cally smooth, uniform, and finer grained compared to a pure zinc coating. The alloy showed high hardness. Comparison of corrosion characteristics of zinc and zinc alloys on steel showed that the latter exhibits superior corrosion resistance. An alloy containing more than 40 wt percent Fe showed good paintability. The optimum bath composition and operating conditions to obtain smooth and uniform alloy deposit with 15–20 wt percent Fe are given in Table 6.

**Editor's note:** Manuscript received, March 1994. Addenda received, August 1996.

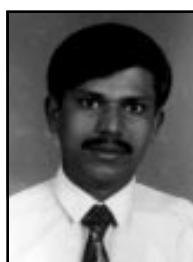
#### Acknowledgment

The authors thank Prof. S.M. Mayanna, chairman, Department of Studies in Chemistry for providing laboratory facilities. One of the authors (V.N.) gratefully acknowledges the CSIR, New Delhi, for financial support.

#### References

1. T. Watanabe, M. Omura, T. Honama and T. Adaniya, *SAE Tech. Paper Series No. 820424*, Detroit, MI (1982).
2. T. Shibuya, T. Kurimoto, K. Korekawa and K. Noji, *Tetsuto-Haganae*, **66**, 771 (1980).
3. R. Noumi, H. Nagasaki, Y. Foboh and A. Shibuya, *SAE Tech. Paper Series No. 820332*, Detroit, MI (1982).
4. T. Kurimoto, Y. Foboh, H. Oishi, K. Yanagawa and R. Noumi, *SAE Tech. Paper Series No. 831837*, Warrendale, PA (1983).
5. T. Adaniya, T. Hara, M. Sagiyama, T. Homa and T. Watanabe, *Plat. and Surf. Fin.*, **72**, 52 (Aug. 1985).
6. F.W. Salt, *Electroplating and Metal Fin.*, **9**, 3 (1956).
7. R. Winand, *Surf. Coating Technol.*, **37**, 65 (1989).
8. S. Sankarapapavinasam *et al.*, *Metal Fin.*, **87**(12), 9 (1989).
9. A. Brenner, *Electrodeposition of Alloys*, Academic Press, Orlando, FL and London, 1963.
10. K. Higashi *et al.*, *J. Electrochem. Soc.*, **128**, 2081 (1981).
11. G.N. Rao and S.C. Rustagi, *Indian J. Chemistry*, **9**(12), 1390 (1971).
12. K. Kondo, J. Ishikawa, O. Takenaka, T. Matsubara and M. Irie, *J. Electrochem. Soc.*, **137**(6), 1859 (1990).
13. S.N. Srimathi and S.M. Mayanna, *Metal Fin.*, **83**(3), 45 (1985).
14. E. Raub and K. Muller, *Fundamentals of Metal Deposition*, Elsevier, New York, NY, 1967.
15. O. Kubaschewski, *Iron Binary Phase Diagrams*, Springer Verlag, New York, NY, 1982; p. 173.
16. M. Hansen, *Constitution of Binary Alloys*, McGraw-Hill Book Co., New York, NY, 1958; p. 737.
17. D. Davidson, *Proc. SAE Int'l Corrosion Congress, Paper No. 860266*, Detroit, MI (Feb. 1986).

#### About the Authors



V. Narasimhamurthy, is a senior research fellow in the Department of Chemistry, Bangalore University, India. He holds BSc and MSc degrees from Bangalore University. His research has been in the field of zinc alloy plating on steel for automotive industrial applications.



Prof. B.S. Sheshadri\* lectures and engages in research at the Department of Studies in Chemistry, Central College, Bangalore University, Bangalore 560 001, India. Currently, he is pursuing research in the area of electrode kinetics, alloy plating and corrosion.

\* To whom correspondence should be addressed.